

New Approach for Determining Tortuosity in Fibrous Porous Media

Rahul Vallabh, Pamela Banks-Lee, Abdel-Fattah Seyam

College of Textiles, North Carolina State University, Raleigh, NC USA

Correspondence To:

Rahul Vallabh, email: rvallabh@gmail.com

ABSTRACT

A method to determine tortuosity in a fibrous porous medium is proposed. A new approach for sample preparation and testing has been followed to establish a relationship between air permeability and fiberweb thickness which formed the basis for the determination of tortuosity in fibrous porous media. An empirical relationship between tortuosity and fiberweb structural properties including porosity, fiber diameter and fiberweb thickness has been proposed unlike the models in the literature which have expressed tortuosity as a function of porosity only. Transverse air flow through a fibrous porous media increasingly becomes less tortuous with increasing porosity, with the value of tortuosity approaching 1 at upper limits of porosity. Tortuosity also decreased with increase in fiber diameter whereas increase in fiberweb thickness resulted in the increase in tortuosity within the range of fiberweb thickness tested.

INTRODUCTION

Fibrous porous media like nonwoven material is an assembly of fibers which are bonded to form coherent structures such as webs, sheets and batts. A characteristic feature of a porous nonwoven material is its high porosity (pore volume fraction). However, in spite of being an open structures, nonwovens have fairly good structural stability which has made nonwovens a preferred choice of material in many barrier applications such as insulation, air filtration and acoustics. Fluid flow properties such as air permeability are of immense importance to the performance of nonwoven materials used in these applications. Fluid flow through a porous medium is influenced by the amount and structure of the void (pore) space. While amount of void space is easily quantified by measurement of porosity,

characterization of void space structure is more difficult due to its complex nature. The actual microscopic path followed by fluid flow through the void space is complicated and is often quantified by the parameter, tortuosity. Determination of tortuosity therefore provides a good understanding of the mechanism of fluid flow and the void space complexity in porous media. Tortuosity is defined in Eq. (1) as the ratio of actual flow path length average, L_e to the length (thickness), L of the porous medium in the direction of macroscopic flow [1-2].

$$\tau = \frac{L_e}{L} \quad (1)$$

Higher value of tortuosity would therefore indicate longer, more complicated and sinuous path thus resulting in greater resistance to fluid flow. Tortuosity also directly influences the heat and electric conductivity, propagation of acoustic waves, filtration and absorbance efficiency in fibrous porous media.

The complex nature of void space within nonwoven materials however, makes it difficult to quantify tortuosity. A simple way to do so would be to assume that a porous medium contains parallel channels of fixed diameter and have their axis inclined at a fixed angle θ to the normal of the porous medium surface. In this case tortuosity τ , would be equal to the inverse of cosine θ . Such a simplified approach however fails to represent the complex nature of the pore channels.

In an early work Piekaar and Clarenburg [2] used geometrical analysis to estimate tortuosity in fibrous porous media. Their proposed model predicts an increase in tortuosity with increasing porosity. The

authors however did not explain the reason for such an unusual behavior. Bo-Ming and Jian-Hua [3] and, Mei-Juan et al. [4] used 2D geometrical analysis to estimate tortuosity of flow path in a porous media with square and spherical particles. Experimental methods using pressure drop measurements across bed of parallelepipedal particles was used by Comiti and Renaud [5] to determine tortuosity with the assumption of shape factor equal to 1. Fella [6] has proposed method involving ultrasonic reflectivity for measuring porosity and tortuosity of porous materials. Such acoustical methods however are only suitable for porous materials with rigid structures. Tortuosity has also been determined experimentally using Nuclear Magnetic Resonance (NMR) measurements [7-8]. However, works involving determination of tortuosity using NMR method are so far limited to non-fibrous porous materials. Models based on diffusion measurements have been proposed for predicting tortuosity in porous materials like soil, sedimentary rocks, solid sediments and sphere packing [9-12]. Electrical resistance measurements have also been used to determine tortuosity of porous materials like Pyrex glass, porcelain, packed activated alumina, packed glass beads, and sandstones by Garrouch et al [13]. Garrouch et al. [13] also list several other models based on electrical resistance measurements, however, validity of models based on electrical resistance measurements has been challenged by Suman and Ruth [14] reasoning that in real porous media, presence of factors like the shape of channels influence the fluid flow unlike electrical flow which only depends upon the total cross-sectional area of channels. Image analysis techniques involving serial sectioning has also been used by Vogel [15] to find pore connectivity, however no attempt was made to determine tortuosity. Tortuosity has also been determined using lattice-gas and random walk simulation results. Koponen et al [1] used lattice-gas simulation in a 2D media to express tortuosity as a function of porosity. Tomadakis and Sotirchos [16] used random-walk simulation results to determine tortuosity as function of porosity, which was used by Tomadakis and Robertson [17] to derive the expression for viscous tortuosity of fibrous porous media with layered microstructure.

Study of previous works has thus shown that very little work has been done to determine tortuosity in fibrous nonwoven materials. Some of the methods used for other types of porous materials are not suitable for fibrous porous materials. A few models have expressed tortuosity in fibrous structures as a function of porosity, while ignoring other variables

like fiber diameter and porous material thickness. The current work involves development of an experimental method for the determination of tortuosity. Relationships between tortuosity and parameters like porosity, fiber diameter and fiberweb thickness have also been established.

DETERMINATION OF PORE CHANNEL TORTUOSITY

In macroscopic terms, Newtonian fluid flow through a porous medium at a low Reynolds number is governed by Darcy's law (Eq. (2)) which states that the flux q (discharge rate per unit area, with units of length per time, m/s) of the fluid is proportional to the pressure gradient ΔP (Pa/m) .

$$q = \frac{-k}{\mu} \Delta P \quad (2)$$

Here, k is the permeability of the porous medium (units of area, m^2) and μ is the dynamic viscosity of the fluid (Pa.s). Using dimensional analysis, it has been suggested that permeability of a porous medium can be expressed by Eq. (3) [1].

$$k = \frac{f(\varepsilon, \tau)}{S^2} \quad (3)$$

Here ε is porosity of the porous medium, τ is the pore channel tortuosity, and S is the specific surface area which is defined as the ratio of total interstitial surface area to the bulk volume of the porous medium. Based on the capillary model which represents a porous material as solid material containing parallel tubes of fixed cross-sectional shape, Carmen-Kozeny equation (Eq. (4)) expresses permeability as a function of porosity ε and hydraulic radius R_h as

$$k = \frac{\varepsilon R_h^2}{c} \quad (4)$$

Here hydraulic radius R_h is equal to ε / S , and c is the Kozeny constant which depends upon the cross section of the tubes. In order to account for the complexity of the actual flow through the porous medium, tortuosity is introduced in the capillary model, in which case permeability is expressed as given by Eq. (5) [1].

$$k = \frac{\varepsilon^3}{c\tau^2 S^2} \quad (5)$$

Permeability of a porous medium is influenced by morphology as well as topology of the pore space structure. In case of fibrous porous medium, morphology and topology of the pore space depends upon the fiber diameter, pore volume porosity and fiber orientation distribution. Porosity and fiber diameter being constant, the thickness of fibrous porous medium does not influence the morphology of the pore structure; however thickness does influence the topological characteristics such as tortuosity. Porosity and fiber diameter being constant, decrease in thickness would cause the fluid flow to follow a less tortuous path, thus resulting in reduced tortuosity. As thickness decreases, the path followed by the fluid flow will become increasingly less tortuous until path becomes almost straight as in the case of nonwoven material with a very small thickness. Using this knowledge of how thickness influences the morphology and topology of pore structure in a porous medium, a new experimental approach has been developed to determine tortuosity of nonwoven porous materials.

Differences in the air permeability of two nonwoven fabrics having the same porosity, fiber diameter and fiber orientation distribution, but having different thickness could be explained by the differences in tortuosity of the fluid flow path in the two porous medium. Tortuosity values τ_1 and τ_2 of two such samples could be related to the respective permeability, k_1 and k_2 as given by Eq. (6).

$$\frac{\tau_1}{\tau_2} = \left(\frac{k_2}{k_1} \right)^{1/2} \quad (6)$$

In the case of nonwoven fabrics with low thickness, where the fluid flow follows almost a straight path, the value of tortuosity could be assumed to be equal to 1. With this assumption, tortuosity $\tau(L)$ of a nonwoven fabric with thickness, L could be determined using Eq. (7).

$$\frac{\tau(L)}{\tau(L)_{L \rightarrow 0}} = \left(\frac{k(L)_{L \rightarrow 0}}{k(L)} \right)^{1/2} \quad (7)$$

Here $\tau(L)$ and $k(L)$ are tortuosity and air permeability respectively of nonwoven fabric with thickness L . $\tau(L)_{L \rightarrow 0}$ and $k(L)_{L \rightarrow 0}$ are the tortuosity and air permeability respectively of nonwoven fabric with very low thickness. Eq. (7) is applicable when both nonwoven fabrics have same porosity, fiber diameter and fiber orientation distribution. Tortuosity, $\tau(L)_{L \rightarrow 0}$ of a nonwoven fabric with low thickness could be assumed to be equal to 1, in which case Eq. (7) can be written as

$$\tau(L) = \left(\frac{k(L)_{L \rightarrow 0}}{k(L)} \right)^{1/2} \quad (8)$$

This approach of determining tortuosity would therefore require establishing a relationship between air permeability and nonwoven fabric thickness. Such an analysis would require a sample set where the thickness is varied at different levels of fiber diameter and porosity. However, due to the production process, fiber diameter, porosity and fabric thickness cannot be independently controlled. In order to overcome this shortcoming, nonwoven fabrics were used in a layered-configuration, which allowed independent control over fabric thickness. The layered-configuration was achieved by layering specimens cut from a sample to form 2-layer, 4-layer and 8-layer configurations. Assuming that each specimen in layered configuration has same porosity, fiber diameter and fiber orientation distribution, pore structure morphology of 2-layer, 4-layer and 8-layer configurations would be the same. The change in thickness however, would result in different tortuosity values associated with the pore structure of these configurations.

SAMPLE DESCRIPTION, METHODS, AND MEASUREMENT OF AIR PERMEABILITY

Samples used in this work included spunbond-calendared, spunbond-needled-calendared, and spunbond-hydroentangled-calendared nonwoven fabrics. Description of fabric samples is shown in *TABLE I*.

TABLE I. Fabric Sample Description

Fabric Sample ID	Description
DP45, DP55, DP68, DP90	DuPont Polypropylene (PP) Spunbond-Calendared
JM1, JM2	Johns Manville Polyester (PET) Spunbond-Needled-Calendered
SB1, SB2	PP Spunbond-Calendared
SBH	PP/PET Core-Sheath Spunbond-Hydroentangled-Calendered

Nonwoven fabric samples were cut into 2.5 inch circular specimens. Due to the non-uniformity in basis weight within a fabric sample, large variation was observed in the basis weight of the specimens cut from a sample. Since a layered configuration would require that each specimen in the configuration has the same porosity, specimens cut from the samples were grouped together according to their basic weights, such that groups of eight specimens having the same or very close basic weights were selected. From these, 2-layer, 4-layer and 8-layer configuration were formed. Each layered configuration was treated as a different sample. A few groups were formed with four specimens instead of eight due to the lack of sufficient specimens with the same basis weights. A total of 112 samples were formed using this method.

Thickness of nonwoven fabric samples (2-layer, 4-layer and 8-layer configuration) measured at pressure of 100 gf/cm², ranged from 0.3 to 4.0 mm. Fiber diameter measured using a microscope and image analysis tool ImageJ, ranged between 7.7 to 25.3 microns. Sample thickness and fiber diameters are listed in TABLE II. As mentioned before the samples obtained from within a single fabric exhibited different porosities due to the local variation in basis weight, therefore for brevity the porosity of the samples are not shown in TABLE II. Porosity of the 112 samples (obtained from all fabrics) ranged from 0.65 to 0.90.

TABLE II. Thickness and Fiber Diameter of Fabric Samples

Fabric Sample ID	Fiber Diameter (μm)	Sample Thickness (mm)		
		2-layer	4-layer	8-layer
SB1	14.3	0.31	0.59	1.08
SB2	15.8	1.00	2.00	4.04
JM1	9.5	0.69	1.33	2.69
JM2	9.5	0.65	1.30	2.63
SBH	7.7	0.89	1.72	3.43
DP45	21.6	0.46	0.90	1.80
DP55	25.3	0.52	1.01	1.95
DP68	25.3	0.56	1.07	2.10
DP90	25.3	0.64	1.24	2.42

Air resistance (Eq. (9)) of 2-layer, 4-layer and 8-layer samples was measured using KES-FS Air-Permeability Tester. Air permeability was determined using sample thickness and measured air resistance using Eq. (10).

$$R = \frac{\Delta P}{v} \quad (9)$$

$$k = \frac{L\mu}{R} \quad (10)$$

Here, R is the measured air resistance (KPa.s/m), ΔP is pressure difference (KPa) across the sample thickness L (m), v is air flow per unit area of sample (m³/m².s), k is the air permeability (m²), and μ is the air viscosity (KPa.s).

Since the structural parameters (factors) could not be positively controlled, a full factorial design of experiments was not possible and therefore statistical analysis software (SAS) was used to establish relationship between air permeability and the structural parameters. Similarly, statistical analysis was also used to establish relationship between tortuosity and structural parameters.

RESULTS AND DISCUSSION

Structural properties of samples and the permeability values determined from the measured air resistance of samples were used to establish an empirical relationship given in Eq. (11).

$$k = 6.82e-06*d(1-\varepsilon)^{-1} - 2.2e-11*\ln(L) + 1.64e-4*d(1-\varepsilon)^2 - 1.71e-9*(1-\varepsilon) - 6.66e-10 \quad (11)$$

Here k is the air permeability (m^2), d is fiber diameter (m), L is sample thickness (m) and ε is porosity. The established empirical equation which is in the form of a linear regression model was established using SAS. The established empirical model had an R-Square value of 0.87 and all variables were found to be significant with at least 99% confidence level. The established empirical model was compared with empirical correlations and analytical models proposed by Davies [18], Koponen et. al [19] and, Tomadakis and Robertson [17].

Davies [18] proposed an empirical correlation by fitting transverse permeability data for flow through highly porous layered fibrous structures, Eq. (12)

$$k = d^2 [64(1-\varepsilon)^{3/2} (1 + 56(1-\varepsilon)^3)]^{-1} \quad (12)$$

where d is fiber radius and ε is the porosity of the fibrous structure. Davies' empirical correlation [18] is valid for porosity, ε greater than 0.7. Tomadakis and Robertson [17] proposed an analytical model, Eq. (13), based on electrical conductivity to predict permeability of fibrous media with layered microstructure.

$$k = \frac{d^2 \varepsilon}{32 \ln^2 \varepsilon} \times \frac{(\varepsilon - \varepsilon_p)^{\alpha+2}}{(1 - \varepsilon_p)^\alpha [(\alpha + 1)\varepsilon - \varepsilon_p]^2}, \quad (13)$$

where d is the fiber diameter, ε is the porosity, ε_p is percolation threshold (0.11) and α is a constant (0.785). Like the model proposed by Davies [18], the analytical model proposed by Tomadakis and Robertson [17] is valid for porosity of media greater than 0.7. Koponen et al [19] used Lattice-Boltzmann method to solve permeability of random 3D fiber web as a function of porosity. The simulated results

were used to obtain the fitted expression given in Eq. (14)

$$k = \frac{d^2}{4} A [e^{B(1-\varepsilon)} - 1]^{-1}, \quad (14)$$

where d is the fiber diameter, ε is porosity, and $A = 5.55$ and $B = 10.1$ are constants. The effect of porosity on permeability is shown in *Figure 1*, which also illustrates the comparison between the empirical relation (Eq. (11)), derived in this research and other empirical and analytical models expressed in Eq. (12) - (14).

Fiber diameter and fiberweb thickness being constant air permeability increased with increasing porosity as expected (*Figure 1*). With respect to relationship between porosity and permeability, the established model (Eq. (11)) showed a similar trend as compared to other models available in the literature (Eq. (12) - (14)). Permeability values estimated by the established empirical model (Eq. (11)) were found to be higher as compared to the values estimated by models proposed by Davies [18] and Koponen et al [19]. Permeability values estimated by the model proposed by Tomadakis and Robertson [17] were also found to be higher than those models proposed by Davies [18] and Koponen et al [19] for porosities greater than 0.90.

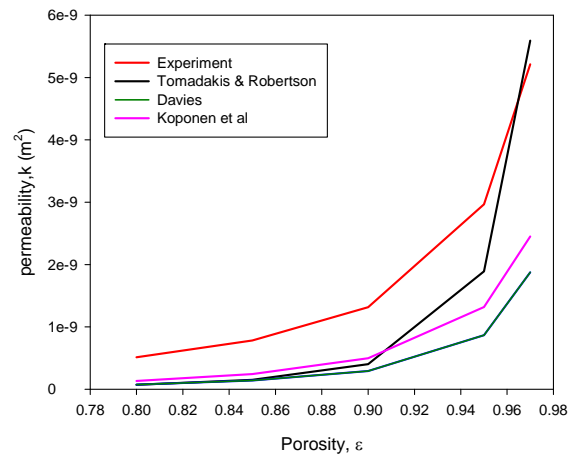


FIGURE 1 Effect of Porosity on Air Permeability at $d = 25$ microns and $L = 5$ mm

Permeability values plotted against fiber diameter in *Figure 2* show that porosity and fiberweb thickness being constant permeability increase with increasing fiber diameter. The plot shown in *Figure 2* also shows that permeability values estimated by the

research model were higher than the values estimated by other models.

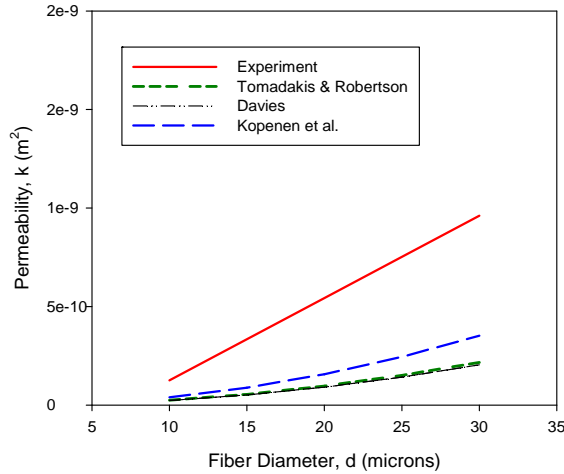


FIGURE 2 Effect of Fiber Diameter on Permeability at $\varepsilon = 0.85$ and $L = 5\text{mm}$

The higher permeability values estimated by the research model can be attributed to the layered configuration of sample. The layered configuration of samples resulted in loss of air flow at the layer interfaces during the air resistivity test which resulted in lower recorded resistivity.

None of the empirical and analytical models found in the literature have investigated the effect of fabric thickness on permeability, however for the range of fabric thickness measured, permeability was found to be significantly influenced by fabric thickness. Therefore, the established empirical model (Eq. (11)) includes fabric thickness as one of the variables, and this formed the basis for determination of tortuosity. Porosity and fiber diameter being constant, permeability of the samples were found to increase with increasing fabric thickness as shown in *Figure 3*.

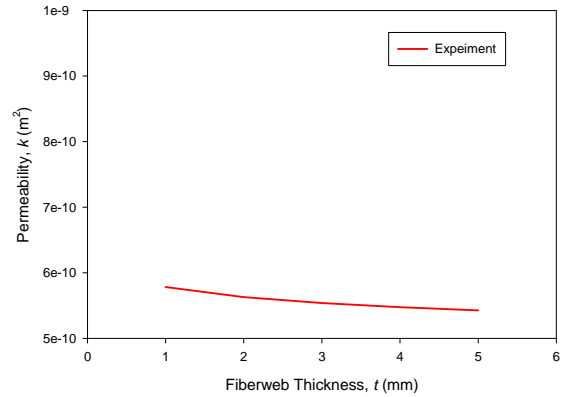


FIGURE 3 Variation of Permeability with Fiberweb Thickness at $\varepsilon = 0.85$ and $d = 20\text{microns}$

Permeability $k(L)$ and the corresponding value of $k(L)_{L \rightarrow 0}$ which are required to determine tortuosity, $\tau(L)$, are calculated using the established empirical relation given by Eq. Value of $k(L)_{L \rightarrow 0}$ was calculated by setting fiberweb thickness, L , equal to 10 times the fiber diameter, d .

Values of tortuosity thus obtained and the structural parameters of the samples were used to establish an empirical relation (Eq. (15)) with the help of statistical analysis software (SAS).

$$\ln(\tau) = -7.83 \ln(\varepsilon) - 0.54 \ln(d) + 0.188 \ln(L) + 4.85 \varepsilon^2 - 4.49, \quad (15)$$

Here τ is the pore channel tortuosity, ε is the porosity, d is the fiber diameter and L is the fiberweb thickness. The empirical relation had a high R-square value of 0.84 and all the variables were found to be significant with at least 99% confidence level.

The established empirical relation is compared with other models for tortuosity proposed by Kopenen et al [1] and, Tomadakis and Sotirchos [16].

Kopenen et al [1] used lattice-gas simulation in a 2D media to determine tortuosity. The simulated values of tortuosity τ , were expressed as function of porosity ε , given by Eq. (16).

$$\tau = 1 + a \frac{(1 - \varepsilon)}{(\varepsilon - \varepsilon_p)^m}, \quad (16)$$

where ε_p is the percolation threshold (0.33), $a = 0.65$ and $m = 0.19$ are constants. Tomadakis and Sotirchos [16] used random-walk simulation results for bulk tortuosity τ_b to establish the correlation given by Eq. (17). Tomadakis and Robertson [17] derived the expression for tortuosity (viscous tortuosity) of fibrous porous media with layered microstructure as a function of porosity ε , and bulk tortuosity τ_b , given by Eq. (18).

$$\tau_b = \left(\frac{1 - \varepsilon_p}{\varepsilon - \varepsilon_p} \right)^\alpha \quad (17)$$

$$\tau = \tau_b \left(1 + \frac{\alpha \varepsilon}{\varepsilon - \varepsilon_p} \right)^2 \quad (18)$$

Here τ_b is the bulk tortuosity, τ is the tortuosity (viscous tortuosity), ε_p is the percolation threshold (0.11) and, α is a constant (0.785). It should be pointed that all the models found in the literature express tortuosity as function of porosity only, while ignoring other structural parameters like fiber diameter and fiberweb thickness.

Relationship between tortuosity and porosity as predicted by the current model (Eq. (15)) and models given by Eq. (16) - (18) is shown in Figure 4.

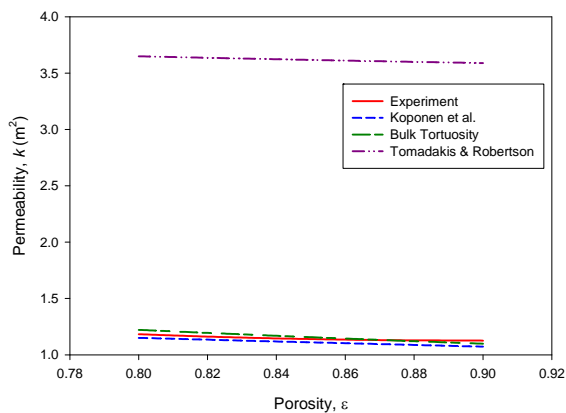


FIGURE 4 Relationship between Porosity and Tortuosity in a Fiberweb, at $d = 20$ microns and $L = 5$ mm

Pore channel tortuosity was found increased with decrease in porosity which is expected as the flow

path becomes longer and more tortuous with decrease in pore volume fraction. With respect to predicting the relationship between tortuosity and porosity, a good agreement was found between the current model (Eq. (15)), the model proposed by Koponen et al. [1] (Eq. (16)) and bulk tortuosity (Eq. (17)). The model proposed by Tomadakis and Robertson (Eq. (18)) [17] dramatically overestimates tortuosity with its value much higher than 1 even at higher porosity.

As mentioned earlier, the models found in the literature have expressed tortuosity as a function of porosity, while ignoring the effect of fiber diameter and fiberweb thickness. The current model expressed in Eq. (15), however showed that both fiber diameter and fiberweb thickness have significant influence on the tortuosity as shown in Figure 5 and Figure 6.

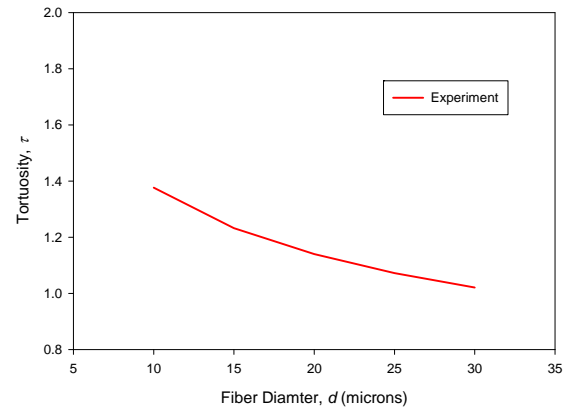


FIGURE 5 Variation of tortuosity with fiber diameter at $\varepsilon = 0.85$, and $L = 5$ mm

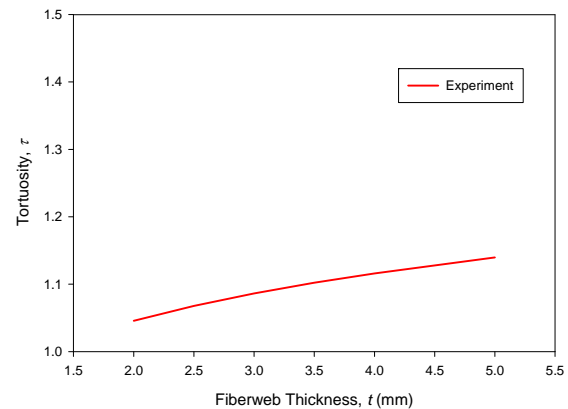


FIGURE 6. Variation of Tortuosity with Fiberweb Thickness at $\varepsilon = 0.85$, $d = 20$ microns

Tortuosity was found to increase as the fiber become finer, with other structural parameters remaining constant (*Figure 5*). As the fiber become finer, the pore space is divided into smaller pore volumes, resulting in the pore channel connecting the pore volumes to be more tortuous.

Porosity and fiber diameter being constant, tortuosity was found to increase with increase in fiberweb thickness (*Figure 6*). In case of very thin fiberwebs, pores on the back and front faces are connected through straight vertical pore channels, however as the thickness of the fiberweb increase the flow path encounters more fibers, thus resulting in more tortuous and longer pore channels connecting the pores on the front and back faces.

CONCLUSIONS

While models available in the literature haven't included fiberweb thickness as a variable affecting permeability, air resistivity experiments showed a significant effect of fiberweb thickness on air permeability. Permeability values estimated by the research empirical model showed that permeability increased with increasing fiberweb thickness with porosity and fiber diameter being constant. With respect to the relationship between permeability and structural properties like porosity and fiber diameter, the research empirical model showed similar trends as compared to the models in the literature. The relationship established between permeability and fiberweb thickness formed the basis for the determination of tortuosity in fibrous porous media using the new approach. With respect to predicting the relationship between tortuosity and porosity, the empirical model developed for tortuosity was in good agreement with other models in the literature which have expressed tortuosity as a function of porosity while ignoring other structural parameters like fiber diameter and fabric thickness. In the current empirical model, structural parameters like porosity, fiber diameter and fabric thickness were found to significantly influence tortuosity. As porosity approached the value of 1, tortuosity reduced to nearly the value of 1 indicating that the pore channels have minimal tortuosity at porosities close to 1. The current empirical model also showed that tortuosity decreased with an increase in fiber diameter, where as it increased with increase in thickness of porous media as expected. The results obtained in this study validate the new approach adopted for determination of tortuosity.

ACKNOWLEDGEMENT

We would like to thank DuPont and Johns Manville for providing samples for this research.

REFERENCES

1. Koponen, A., Kataja, M., Timonen, J, *Simulations of Single-Fluid Flow in Porous Medium*. International Journal of Modern Physics, 1998. **9**(8): p. 1505-1521.
2. Piekhaar, H.W., Clarenburg, L.A, *Aerosol Filters- the Tortuosity Factor in Fibrous Filters*. Chemical Engineering Science, 1967. **22**: p. 1817-1827.
3. Bo-Ming, Y., Jian-Hua, L, *A Geometry Model of Tortuosity of Flow Path in Porous Media*. Chinese Physics Letters 2004. **21**(8): p. 1969-1971.
4. Mei-Juan, Y., Bo-Ming, Y., Bin, Z., Ming-Tao, H, *A Geometry Model for Tortuosity of Streamtubes in Porous Media with Spherical Particles*. Chinese Physics Letters, 2005. **22**(6): p. 1464-1467.
5. Comiti, J., Renaud, M, *A New Method for Determining Mean Structure Parameters of Fixed Bed from Pressure Drop Measurements: Application to Bed Packed with Parallelepipedal Particles*. Chemical Engineering Science 1989. **44**(7): p. 1539-1545.
6. Fellah, Z.E.A., *Direct and inverse Scattering of Transient Acoustic Waves by a Slab of Rigid Materials*. Journal of the Acoustical Society of America, 2003. **113**(1): p. 61.
7. Rigby, S.P., Gladden, L.F, *NMR and Fractal Modelling Studies of Transport in Porous Media*. Chemical Engineering Science, 1996. **51**(10): p. 2263 - 2272.
8. Wang, R., Pavlin, T., Rosen, M.S., Mair, R.W., Cory, D.G., Walsworth, R.L, *Xenon NMR Measurements of Permeability and Tortuosity in Reservoir Rocks*. Magnetic Resonance Imaging, 2005. **23**: p. 329-331.
9. Boving, T.B., Grathwohl, P, *Tracer Diffusion Coefficient in Sedimentary Rocks: Correlation to Porosity and Hydraulic Conductivity*. Journal of Contaminant Hydrology, 2001. **53**: p. 85-100.
10. Moldrup, P., Olesen, T, Komatsu, T, Schjonning, P, Rolston, D.E, *Tortuosity, Diffusivity, Permeability in the Soil Liquid and Gaseous Phases*. Soil Science Society of America Journal, 2001: p. 613 - 623.
11. Brakel, J.V., Heertjes, P.M., *Analysis of Diffusion in Microporous Media in Terms of a Porosity, a Tortuosity and a Constrictivity Factor*. International Journal of Heat and Mass Transfer 1974. **17**: p. 1093-1103.
12. Boudreau, B.P., *The Diffusive Tortuosity of Fine-Grained Unlithified Sediments*. Geochimica et Cosmochimica Acta, 1996. **60**(16): p. 3139-3142.
13. Garrouch, A.A., Ali, L., Qasem, F, *Using Diffusion and Electrical Measurements to Assess Tortuosity of Porous Media*. Industrial Engineering and Chemical Research 2001. **40**(20): p. 4363 - 4369.
14. Suman, R., Ruth, D, *Formation Factor and Tortuosity of homogeneous Porous Media*. Transport in Porous Media, 1993. **12**: p. 185-206.
15. Vogel, H.J., *Morphological Determination of Pore Connectivity as a Function of Pore Size using Serial Sectioning*. European Journal of Soil Science, 1997. **48**: p. 365-377.
16. Tomadakis, M.M., Sotichos, S.V, *Ordinary and Transition Regime Diffusion in Random Fiber Structures*. American Institute of Chemical Engineers Journal, 1993. **39**(3): p. 397-412.
17. Tomadakis, M.M., Robertson, T.J, *Viscous Permeability of Random Fiber Structures: Comparison of Electrical and*

- Diffusional Estimates with Experimental and Analytical Results*. Journal of Composite Materials, 2005. **39**: p. 163-188.
18. Davies, C.N. *The Separation of Airborne Dust and Particles*. in *Proceedings of Institute of Mechanical Engineers*. 1952. London.
19. Koponen, A., Kandhai, D., Hellen, E., Alava, M., Hoekstra, A., Kataja, M., Niskanen, K, *Permeability of Three-Dimensional Random Fiber Webs*. Physical Review Letters, 1998. **80**(4): p. 716-719.

AUTHORS' ADDRESS

Rahul Vallabh, Ph.D.

Pamela Banks-Lee, Ph.D.

Abdel-Fattah Seyam, Ph.D.

North Carolina State University
2401, Research Drive, Box 8301
Raleigh, NC 27695